IDEFIX · Identification of dental fixtures in intraoral X rays*

Thomas Lehmann[1], Walter Schmitt[2], Harald Horn[1], Walter Hillen[3]

[1]Institute of Medical Informatics and Biometry
[2]Clinic for Oral, Maxillofacial, and Facial Plastic Surgery
The Aachen University of Technology (RWTH), D-52057 Aachen, Germany
[3]Department of Medical Engineering
Technical College Aachen, D-52428 Jülich, Germany
Email: lehmann@vaire.imib.rwth-aachen.de

ABSTRACT

In dental implantology more than one hundred enossal implant systems are in use. Once embedded, the dental X–ray examination is the most important tool for determing implants' producer, name, and type. In this paper, we present a system for automatical detection and identification of dental fixtures in intraoral X rays (IDEFIX) combining common direct digital image acquisition techniques with specially designed image analysis. IDEFIX can process any digital radiograph (e.g. RVG, Sens-A-Ray, Schick, Sidexis, Digora) as well as digitized dental films.

A reference database has been generated by precise measurement on the implant systems used so far (eight implants) including parameters like length, diameter, and cross section area. After binarization of the current digital X–ray image, a parameter set is extracted from each detected object applying mathematical morphology. All objects are classified using a simplified nearest neighbor method and the Euclidean distance metric. If the distance of the objects' parameter set to one of the reference sets is below a given threshhold, name and type of the identified dental fixture are displayed on the screen. Otherwise, the actual object will be rejected as a non–implant.

IDEFIX has been evaluated by processing various in–vitro acquired radiographs. Different implants were classified captured with identical conditions as well as acquired varying the angulation of the X–ray tube. It is shown that misangulations up to twenty degree are tolerable preserving correct identification. Other image structures like teeth or fillings result in large distances to all reference parameter sets and therefore, they are reliably recognized as non–implants.

Keywords: Medical Imaging, X–Ray Imaging, Dental Radiology, Direct Digital Radiography, Computer Assisted Diagnosis, Digital Image Processing, Pattern Recognition, Object Identification, Threshholding, Mathematical Morphology

*This study was part of the project *Free–hand Subtraction Radiography*. The support of the German Research Community (DFG grant No. Re 427/5–1) is greatfully acknowledged.

0-8194-2085-9/96/$6.00

1 INTRODUCTION

Dental implantology has been established over the past few years as a reliable method for replacing lost teeth. Cylindrical titanium implants, usually screws, are embedded in the jawbone and crowns, bridgeworks or dentures are fixed onto these. Nowadays, there are more than one hundred enossal implant systems in use with respective different types. Therefore, it is difficult for the examiner to correctly determine the implant model and its producer only by means of intraoral acquired radiographs, especially when implant patients change their dentists. For identification, the examiner analyses the two–dimensional shape resulting from X–ray projection of the three–dimensional implant.

In the field of computer vision and image processing, mathematical morphology has been proven to be most useful in shape analysis. The theory of morphology developed by *Serra*,[1] *Steinberg*,[2] and *Haralick*[3,4] provides an orderly method for decomposing global geometric measurements into sequences of local and therefore fast transformations. In other words, mathematical morphology provides an algebraic formulation for applying neighborhood operations to images. Both, the binarized X ray and the structuring element are considered as sets of points and the sequence of different structuring elements applied to an image gives rise to geometric measurements.

Although geometric measurement is a frequent task in medical image processing, only a few applications of mathematical morphology are published in this field, e.g. for edge detection[5] or segmentation.[6,7] There are three major reasons for the complication combining mathematical morphology with medical image processing. Firstly, the binarization of medical images like ultrasonics, histological slices, CTs, MRs, or X rays is difficult. Usually, there is no unitary border confining biological objects in such images. Secondly, the shape of objects may vary in successively recorded images or from patient to patient. This complicates the design of structuring elements. Last but not least, medical imaging is often false to scale. Due to the central projection, the relation between the size of picture elements and the objects depends on the object–film distance and may not be given in general.

Considering intraoral X–ray images, the focus implant distance is fixed by the tube touching the patient's face. Either the patient is asked for assistance or a stent is used to press the film or CCD–sensor onto jaw and teeth yielding a constant implant–film distance. Therefore, a unitary scale can be measured for each intraoral imaging system like RVG, Sens-A-Ray, Schick, Sidexis, or Digora. Furthermore, a scale can be given for every scanning system digitizing dental films. In addition, dental fixtures are machined so that their shapes figured in radiographs may differ only due to projection. This enables the union of mathematical morphology and medical image processing for the automatical detection and identification of dental fixtures in intraoral X rays (IDEFIX). The geometric measures extracted by morphological shape analysis of binarized dental radiographs were compared to those accurately measured on the implants. Thus, a robust implant recognition and identification is possible.

A general implant model is presented in the next section to define the parameters included in the reference database. In Section 3, morphologic image processing is discussed in detail. After scaling (Section 3.1) and binarization (Section 3.2) three sequences of structuring elements are applied extracting global, internal, and external features (Sections 3.3, 3.4, and 3.5, respectively). The application of IDEFIX to various in–vitro radiographs is described in Section 4 and the results are discussed in the last chapter of this paper.

2 REFERENCE DATABASE

Enossal implants are most frequent used in dental implantology. Not only srews and cylinders, but also hollow cylinders, leafs, and pins are implanted. The great variety of enossal dental implants is described elsewhere.[8,9] Nevertheless, every implant can be characterized by the abstract implant model shown in Figure 1. Based on this model, implants are described by their cross section area A_O, length l and averaged diameters at top, middle, and bottom d_1, d_2, and d_3, respectively. All implants must have an internal thread at top with the cross section area

normalized parameter			X_1	X_2	X_3	X_4	X_5	X_6
implant system	j	type	l	A_O	c	s	A_B	A_L
APA–ceram	1	cylinder	0.00	0.09	0.46	0.16	0.75	0.00
Bonefit	2	screw	1.00	0.46	0.60	0.54	0.67	0.00
Bonelock	3	screw	0.77	0.00	1.00	1.00	0.00	0.00
Branemark	4	screw	0.37	0.11	0.49	0.51	0.67	0.11
Frialit II	5	cylinder	0.61	0.54	0.84	0.34	0.72	0.00
ITI–cylinder H	6	cylinder	0.48	1.00	0.00	0.00	0.00	1.00
IMZ–implant	7	cylinder	0.40	0.28	0.51	0.33	1.00	0.29
TPS–screw	8	screw	1.00	0.35	0.71	0.85	0.16	0.00

Table 1: REFERENCE DATABASE
The table on the left shows the reference database, generated by precise measurements of all implant systems followed by normalization to the range between zero and one. Eight implant systems have been included so far, four screws and four cylinders. The normalized parameters are denoted by X_i with $1 \leq i \leq 6$.

A_B to fix the denture. Screws are also determined by the number of thread series t. In addition, some implants may have drill holes through their bottom to prevent rotations of the implant in the bone. The cross section area of those rotation locks A_L is used to distinguish implants, too. Furthermore, implants are characterized by their conical shape c and length–to–diameter ratio s

$$c = \frac{d_1}{d_3}, \qquad s = \frac{l}{\bar{d}}, \qquad \text{with} \qquad \bar{d} = \frac{1}{3}\left(d_1 + d_2 + d_3\right) \tag{1}$$

Based on eight implant systems, four screws and four cylinders, a reference database has been generated (Tab. 1). After precise measuring the implants, all values have been normalized to the range between zero and one. IDEFIX extracts the same parameters from all binary objects in the current digital X ray using morphological image analysis. After introducing mathematical morphology special designed image processing and object classification are discussed in the following chapter.

3 DIGITAL IMAGE PROCESSING

There are several textbooks introducing to mathematical morphology,[10–13] but also using different terminologies. The language of mathematical morphology used here is that of set theory according to *Haralick*.[14] The set of all black pixels in a binary image constitutes a complete description of the black and white image Z^2. In general,

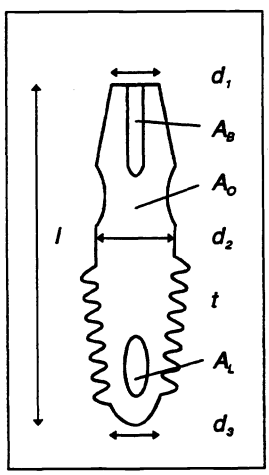

Figure 1: IMPLANT MODEL
Abstracting their outline, dental implants may be characterized by the cross section area A_O, length l, and diameters averaged at top, middle, and bottom, d_1, d_2, and d_3, respectively. All implants have an internal thread at top to fix the denture, but only some implants have drill holes in their bottom, too. These drillings are to avoid rotations. The cross section areas of threaded bushings A_B and rotation locks A_L as well as the number of external thread series t are also used to distinguish implant systems.

the image I and the structuring element E are sets in Z^N with elements i and e, respectively, $i = (i_1, \ldots, i_N)$ and $e = (e_1, \ldots, e_N)$ being N–tuples of element coordinates, then the erosion of I by E, denoted by $I \ominus E$, is defined by

$$\begin{aligned} I \ominus E &= \{x \in Z^N \,|\, \text{for every } e \in E, \text{ there exists an } i \in I \text{ such that } x = i - e\} \\ &= \{x \in Z^N \,|\, (E)_x \subseteq I\} \quad \text{with} \quad (E)_x = \{c \in Z^N \,|\, c = e + x \text{ for every } e \in E\} \end{aligned} \tag{2}$$

In other words, the erosion of an Image I by a structuring element E is the set of all elements $x \in Z^N$ for which E translated to x is completely contained in I. The dilation of I by E

$$I \oplus E = \{x \in Z^N \,|\, (\hat{E})_x \cup I \neq \emptyset\} \qquad \text{with} \qquad \hat{E} = \{x \in Z^N \,|\, x = -e \text{ for every } e \in E\} \tag{3}$$

is the set of all elements $x \in Z^N$ for which E translated to x and I have at least one consolidated element coordinate. In practice, dilations and erosions are usually employed in pairs. Therefore, the opening and closing of I by E is denoted by $I \circ E$ and $I \bullet E$, respectively, with $n \geq 1$ being the integer number of iterations

$$(I \circ E)^{(n)} = \left((I \ominus E)^{(n)} \oplus E\right)^{(n)} \qquad \text{and} \qquad (I \bullet E)^{(n)} = \left((I \oplus E)^{(n)} \ominus E\right)^{(n)} \tag{4}$$

Equations 2 to 4 demonstrate the structuring element E determining the result of morphologic image processing. In spite of filter design in linear system theory, e.g. low–pass filtering for noise reduction, where the coefficients of the filter mask are deduced from theory, the shapes of structuring elements are somewhat arbitrary. Although strategies composing structuring elements are described in textbooks and theory of optimal structuring element decomposition is well known,[3] the performance of mathematical morphology depends on the engineer's experience. Figure 2 summarizes the structuring elements $E_i, 1 \leq i \leq 7$, used in the IDEFIX system.

3.1 Scaling

Before binarization, the gray value images are resized by 4×4 bicubic spline interpolation[15,16] (Fig. 3a,b). This is not only to reduce computing time, but also to make IDEFIX independent of the picture's origin. Therefore, the scale is adapted to the imaging system. The absolute pixel size is a priori known for each recording system. The fixed scale resulting for IDEFIX's image analysis is 5 lp/mm which equals a pixel size of 100 μm. Thus, any digital intraoral imaging system as well as digitized dental films can be processed.

3.2 Binarization

To apply mathematical morphology for shape analysis, the pictures have to be binarized. This is usually done with thresholding techniques.[17,18] Although the histogram bimodality analysis proposed by *Otsu*[19] has been proven to be superior to other techniques,[17,18] it is not useful to extract implants in dental radiographs. Implants, bone, and teeth are usually merged to one segment. To avoid undersegmentation, the threshholding

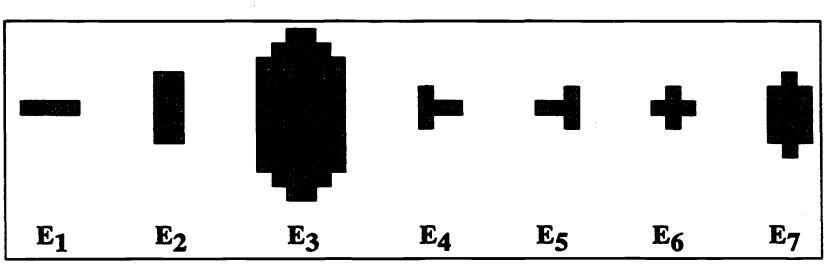

Figure 2: STRUCTURING ELEMENTS Seven structuring elements are applied to binary objects for geometric measurements. They are subsequent denoted by E_i with $1 \leq i \leq 7$.

proposed by *Otsu* is applied local with a window size w corresponding to the average implant diameter $\bar{d}$. Referring to the implant model (Fig. 1) the diameter $\bar{d}$ in (1) of most implants is about 3mm. Taking into account IDEFIX's fixed scale yields $w = 29$. Now, the resulting binary image (Fig. 3c) represents any implant as a connected segment regardless of whether it is adjoining to bone or soft tissue. Note the wide gap surrounding the implant Figure 3c.

Binary erosion (2) is used to supress salt and pepper noise resulting from the spongy structures of the jawbone (Fig. 3d)

$$I_2 = I_1 \ominus E_3 \tag{5}$$

with I_1 denoting the binarized radiograph (Fig. 3c) and E_3 defined in Figure 2. The set E_3 is similar to the shape of implants and its size is choosen expecting the implants to be dominate structures in dental radiographs. Although small segments are dropped after erosion, usually more than one object is retained (Fig. 3e). After labelling, each object can be addressed and sequentially processed.

The retained objects must be extracted and adjusted before geometric measures can be determined. This processing is demonstrated in Figure 4 for two objects taken from Figure 3e, the branemark screw (top line) and the part of the front teeth (bottom line). At first, the object to be adjusted is suppressed in the labelled image denoted by I_2'. To extract the object of interest, I_2' is dilated by E_3 (Fig. 4a,e) and subtracted from I_2 (Fig. 4b,f)

$$I_3 = I_2 - (I_2' \oplus E_3) \tag{6}$$

After labelling I_3, the object is located and extracted using a memorized element coordinate from the dropped subset (Fig. 4c,g). Geometric measurements are simplified adjusting the isolated object into its standard position by the main axis transformation which is also referred to as Karhunen–Loève transform (Fig. 4d,h). The result of adjustment is subsequently denoted by I_4.

Shape analysis by mathematical morphology is applied to the isolated and adjusted objects. The three filters designed for assessing global, internal and external object features are described in the following paragraphs.

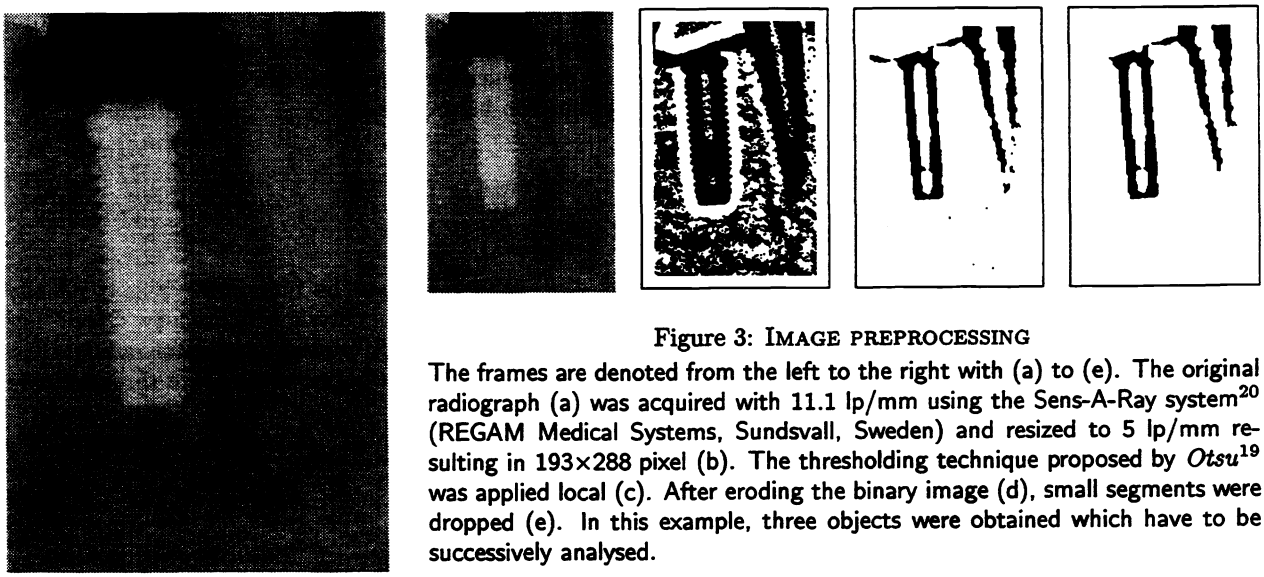

Figure 3: IMAGE PREPROCESSING
The frames are denoted from the left to the right with (a) to (e). The original radiograph (a) was acquired with 11.1 lp/mm using the Sens-A-Ray system[20] (REGAM Medical Systems, Sundsvall, Sweden) and resized to 5 lp/mm resulting in 193×288 pixel (b). The thresholding technique proposed by *Otsu*[19] was applied local (c). After eroding the binary image (d), small segments were dropped (e). In this example, three objects were obtained which have to be successively analysed.

3.3 Global implant structures

Before the global measures A_O, l, and d_i are allowed to be determined by simple counting the number of pixels, the current object is internal closed and its outline is smoothed applying morphologic opening (Fig. 5)

$$I_{\text{glob}} = \Big(\big(I_4 \bullet E_6 \big) \circ E_2 \Big)^{(3)} \tag{7}$$

The structuring element E_6 used for internal closing approximates a disk while E_2 used for opening the outlines is designed to destroy vertical orientated structures like threads. Equation (7) is exampled in Figure 5 with I_{glob} corresponding to Figure 5c.

3.4 Internal Implant Structures

To obtain the internal measures A_B and A_L the object is subtracted from the internal closed object. Before measuring on the internal shapes, smoothing is required

$$I_{\text{int}} = \Big(\big(\big(I_4 \bullet E_6 \big) - I_4 \big) \ominus E_1 \Big) \oplus E_7 \tag{8}$$

Again, this is done with erosion followed by dilation, but this time the structuring elements used for erosion and dilation differ. The erosion is applied to separate drillings which may be merged during binarization. Therefore, the horizontally orientated thin structuring element E_1 is choosen. To preserve the original dimension of internal structures dilation is required using the structuring element E_7 similar to the expected shape of drillings. This is demonstrated in the right part of Figure 5 with I_{int} corresponding to Figure 5f.

Whether the number of object pixels in I_{int} is added to A_B or A_L depends on the object's center of mass lying above or below the center of mass of the internal closed object, respectively.

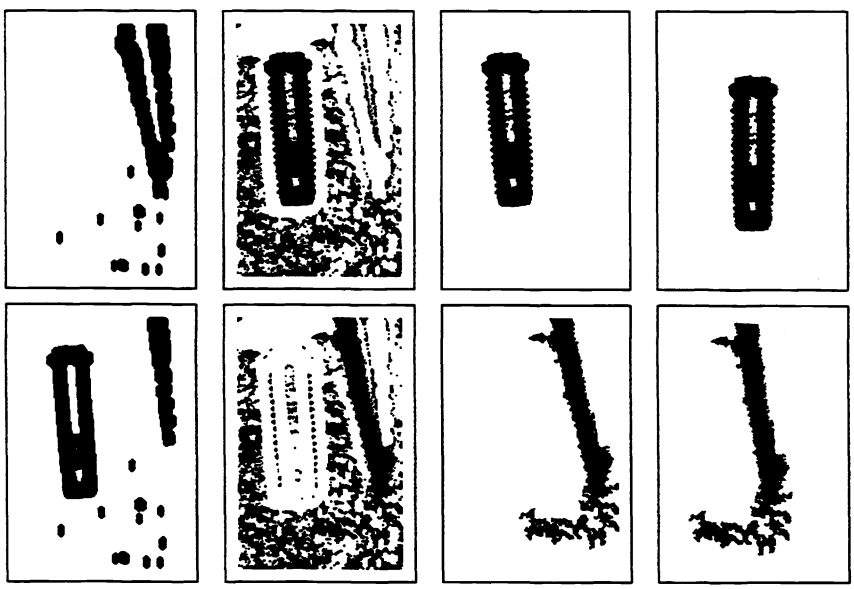

Figure 4: SELECTING OBJECTS
The frames are denoted from left to right by (a) to (d) and (e) to (h) for top and bottom line, respectively, with each line demonstrating the adjustment of one segment taken from Figure 3. After labelling, the current segment is dropped and all maintaining structures are dilated by E_3 (a,e). The result is subtracted from the binary image before erosion (b,f). Using any pixel position from the dropped segment, the object is selected (c,g) and subsequently moved into its standard position (d,h) by the main axis transformation.

3.5 External implant structures

The third sequence of morphologic filters was designed to extract the number of threads t. The object's border I_5 is extracted subtracting the same smoothed object I_{glob}. Note that I_{glob} is used before to global measure the internal closed object. To distinguish between screws and cylinder implants, the structuring elements E_4 and E_5 were designed to model right and left side of threads, respectively. Therefore, in

$$I_{\text{ext}} = (I_5 \ominus E_4) \cup (I_5 \dot{\ominus} E_5) \qquad \text{with} \qquad I_5 = (I_4 \bullet E_6) - I_{\text{glob}} \tag{9}$$

each thread is represented as a separated object. The number of connected components retaining in I_{ext} indicates the current object being a screw or cylinder.

Figure 6 exemplifies this procedure. Although the Branemark screw exhibits only very small threads (Fig. 6a), they are carefully preserved by the respective morphologic filtering for left and right directed structures (Fig. 6f). On the other hand, all segments caused by the roughness of the APA–cylinder (Fig. 6g) are steady removed applying mathematical morphology (Fig. 6l).

3.6 Classification

Based on the morphological processed images I_{glob}, I_{int}, and I_{ext} defined in (7), (8), and (9), respectively, the measures X_i^{mes} corresponding to X_i^{ref} included in the reference database (Tab. 1) are determined easily by counting the number of pixels. Regarding to the number of threads t, the current object is grouped to screw or cylinder systems, if $t > t_T$ or $t \leq t_T$, respectively. Without limiting the general validity, the threshold $t_T = 3$ can be deduced from Figure 6. The binarization of the radiographs sometimes produces two artefacts at the top corners of the implants and therefore, t_T should be larger than two.

The squared unstandardized Euclidean distance[21]

$$D_j = \sum_{i=1}^{6} \left(X_i^{\text{ref}} - X_i^{\text{mes}} \right)^2 \tag{10}$$

to all systems j of the respective group is calculated and the current object is classified using the nearest neighbor

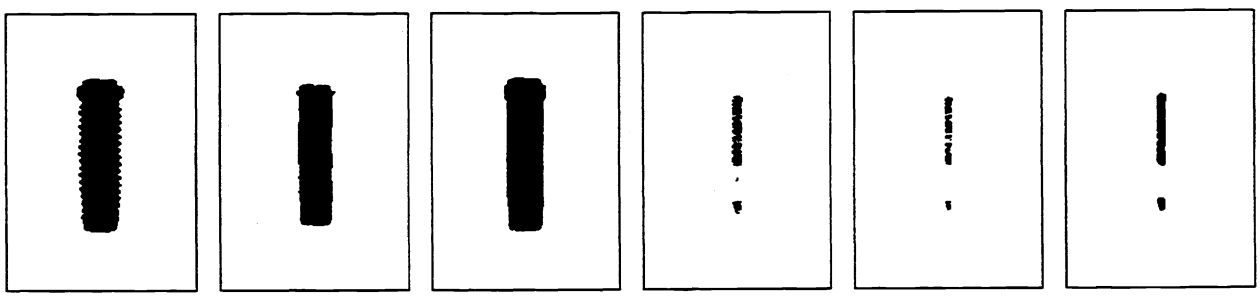

Figure 5: GLOBAL AND INTERNAL MEASURES
The frames are denoted from left to right by (a) to (f). The adjusted object (Fig. 4d) is internal closed (a) preserving the outlines which are succeeding smoothed combining erosion (b) and dilation (c). Global measures like length, diameter, or area can now easily be counted. Subtracting the adjusted object (Fig. 4d) from the internal closed one (a) extracts internal structures (d). Before measuring, they are smoothed by erosion (e) and dilation (f).

approach

$$D_{\min} = \min_j \{D_j\} \tag{11}$$

If $D_{\min}$ is below the threshold D_T, name, producer, and type of the identified implant is displayed on the screen. Otherwise, the current object is certainly rejected as a non–implant.

4 IN–VITRO STUDIES

To evaluate the IDEFIX system, three in–vitro studies were designed. At first, the capability to detect and identify dental implants was evaluated. Next, the correct classification of non–implants was proved and last but not least, the results identifying fixtures captured with different X–ray projections were checked.

4.1 Identification of dental fixtures

The fixtures used to create the reference database (Tab. 1) were radiographed with identical conditions (Fig. 7). Therefore, all implants, except the ITI–cylinder, were fixed successively at the same position on a dry mandible with teeth and fillings and captured keeping geometric projection and X–ray dose. Because of its size, the ITI–cylinder was placed on another human jaw without continuous teeth. In the resulting radiographs the spongy structure of bone is overlayed to the threads of the fixture complicating the classification problem.

The resulting distances D_j are summarized in Table 2. All implants are correctly grouped as screws or

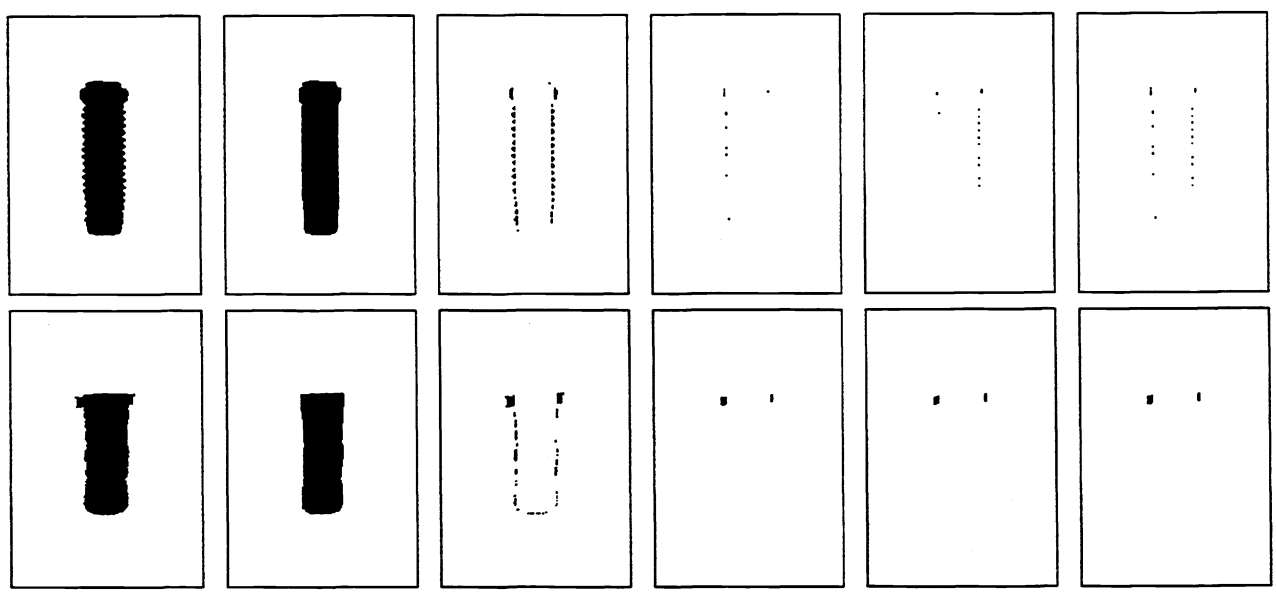

Figure 6: EXTERNAL MEASURES
The frames are denoted from left to right by (a) to (f) and (g) to (l) for the top and the bottom line, respectively. Robust detection of threads is required to differentiate screws and cylinder implants. Subtracting the eroded object (b,h) from the internal closed object (a,g) allows the assessment of threads (c,i). The number of connected components maintaining in the union (f,l) of erosion with a left (d,j) and right (e,k) orientated structuring elements indicates the number of threads.

Distances for	cylindrical implants				implant screws			
implant system	D_1	D_5	D_6	D_7	D_2	D_3	D_4	D_8
APA–ceram	**0.05**	0.72	2.53	0.49	–	–	–	–
Bonefit	–	–	–	–	**0.05**	0.81	0.62	0.18
Bonelock	–	–	–	–	1.33	**0.03**	1.41	0.43
Branemark	–	–	–	–	0.58	0.82	**0.09**	0.65
Frialit II	1.08	**0.05**	2.35	0.58	–	–	–	–
ITI–cylinder H	2.84	2.40	**0.03**	2.29	–	–	–	–
IMZ–implant	0.37	0.22	1.92	**0.15**	–	–	–	–
TPS–screw	–	–	–	–	0.52	0.27	1.07	**0.01**

Table 2: IDENTIFICATION OF DENTAL FIXTURES
The table on the left shows the distances D_j defined in (10). They are calculated for the implant systems which have been radiographed with equal conditions (Fig. 7). The bold faced numbers indicate all implants to be correctly identified.

cylinders. This is marked by the dashed lines. Note that the implant systems are sorted alphabetically and therefore, $j = 1$, 5, 6, and 7 indicates cylinders while $j = 2$, 3, 4, and 8 names screws. The smallest distance in each group is bold faced proving exact recognition. The distances to the corresponding reference parameters $D_{\min}$ are usually smaller than 0.1 but the distances to the other reference parameter sets D_j range from 0.2 up to 2.5. This points out the robustness of the IDEFIX system.

4.2 Classification of non–implants

Our first study proves IDEFIX's sensitivity detecting implants in dental radiographs and its reliability determining the implants' producer, name, and type. This study was designed to assess the specificity discerning dental fixtures and other structures. Four test objects resulting from binarization of dental X–ray images (Fig. 8) where arbitrary choosen and classified with IDEFIX.

The measured distances D_j are shown in Table 3. All segments are grouped as screws because of their ragged outline. The distances to all reference parameter sets D_j range from 1.3 up to 5.3. Therfore, all test objects are

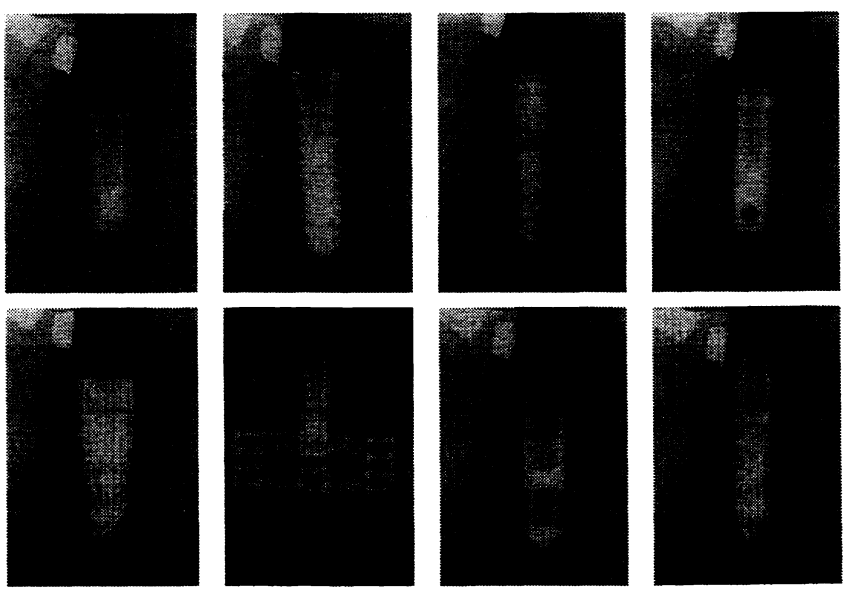

Figure 7: IDENTIFICATION OF DENTAL FIXTURES
The implants are sorted alphabetically from left to right and from top to bottom: APA–ceram, Bonefit, Bonelock, Branemark, Frialit II, ITI–cylinder H, IMZ–implant, and TPS–screw. All implants are captured with identical conditions.

Distances for test objects	cylindrical implants				implant screws			
	D_1	D_5	D_6	D_7	D_2	D_3	D_4	D_8
structure Fig. 8a	–	–	–	–	3.78	2.40	4.22	2.45
structure Fig. 8b	–	–	–	–	5.30	2.56	5.22	3.95
structure Fig. 8c	–	–	–	–	1.97	1.36	2.53	1.49
structure Fig. 8d	–	–	–	–	3.08	3.46	1.69	3.26

Table 3: CLASSIFICATION OF NON–IMPLANTS
This table shows the distaces D_j calculated for the test objects arbitrary taken from clinical radiographs (Fig. 8). The lower limit 1.36 of D_j proves IDEFIX to be specific.

classed as non–implants. Furthermore, the threshold D_T to accept the current object to be an implant or not could be set in the wide range $0.5 < D_T < 1.0$ without changing the classification results.

4.3 Invariance to projection

The third study was done to judge the identification of implants acquired with clinical conditions. Conserving the sensor–implant distance about 1cm, the projection was modified by rotating the X–ray tube along the implant axis up to 20 degrees in steps of 5°. Again, a dry mandible was used to figure spongy structures. In every angulation, all implants were radiographed and processed.

With 0° and 5° angulation, all implants were correctly identified. With 10° the threads of Branemark screws are weakly figured and therefore, the Branemark is sometimes grouped to cylinders depending on dose and underlying bone structures. The same problem arises for TPS–screws commencing with 15°. In such cases, screws are recogniced as cylinders but at least not rejected as non–implants. Captured with 20°, screws like Bonefit and Bonelock are identified with distances $D_{\min}$ equal to 0.07 and 0.04, respectively. Only once, the IMZ–implant was named as Frialit with $D_5 = 0.16$ and $D_7 = 0.18$ while all other cylinders were exactly recogniced.

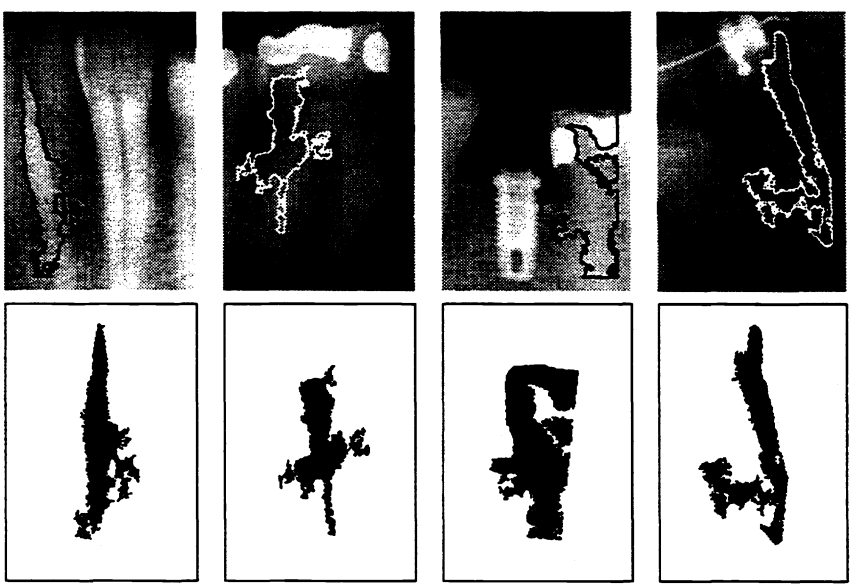

Figure 8: CLASSIFICATION OF NON–IMPLANTS
The images are denoted from left to right by (a) to (f) and (g) to (l) for the top and the bottom line, respectively. The objects classified with IDEFIX were arbitrary choosen from some clinical radiographs. The contours resulting from binarization are surrounded in the images (a) to (f) by a white or black line. Their adjusted shapes used for morphological measurements are respective figured in the frames (g) to (h).

5 CONCLUSION AND DISCUSSION

In this paper, we presented a system for automatic detection and identification of dental fixtures in intraoral X rays (IDEFIX). Several image features are extracted by digital image processing from direct digital acquired radiographs. The unusual combination of mathematical morphology and medical imaging is enabled by the specific imaging geometry in intraoral radiology.

Various in–vitro captured radiographs were processed proving IDEFIX's sensitivity detecting implants, its specificity identifying implants, and its reliability rejecting non–implants. Problems may occure, if implants are X–rayed by a more than 15° angulated tube. In this case, small thread series being existent by Branemark and other implants, are merged to the implant body during binarization. This can be avoided, if adaptive image restoration is applied before binarization.[22] Nevertheless, an angulation of the X–ray tube about 20° is unusual in clinical radiographs and therefore, varying projection is not restrictive for IDEFIX.

IDEFIX is a further step forward to computer assisted diagnosis of dental radiographs. The extension of the fixtures database to additional implant systems, followed by the identification of more complex pattern like teeth, bone, or cavities is the aim of further research.

The recognition and exact localization of dominant image structures, e.g. the implants' center of gravity, can also be used to generate corresponding points whenever radiographs of the same dental region are to be compared.[23] One matching point per image allows the registration of pure translations. At least four of those reference points are required to correct geometrical differences according to the model of perspective projection. The registration of images permits their subtraction simplifying the detection of local changes in hard tissues.

6 REFERENCES

1. J. Serra, "Introduction to Mathematical Morphology," *Computer Vision, Graphics, and Image Processing,* Vol. 35, pp. 283–305, 1986.
2. S. R. Sternberg, "Grayscale Morphology," *Computer Vision, Graphics, and Image Processing,* Vol. 35, pp. 333–355, 1986.
3. X. Zhuang, R. M. Haralick, "Morphological Structuring Element Decomposition," *Computer Vision, Graphics, and Image Processing,* Vol. 35, pp. 370–382, 1986.
4. R. M. Haralick, S. R. Sternberg, X. Zhuang, "Image Analysis Using Mathematical Morphology," *IEEE Trans. on PAMI,* Vol. PAMI–9, pp. 532–550, July 1987.
5. S. Godbole, A. Amin, "Mathematical Morphology for Edge and Overlap Detection for Medical Images," *Real–Time Imaging,* Vol. 1, pp. 191–201, 1995.
6. C.-C. Ko, C.-W. Mao, Y.-N. Sun, S.-H. Chang, "A fully automated identification of coronary borders from tree structure of coronary angiograms," *Int. Journal of Bio–Medical Computing,* Vol. 39, pp. 193–208, 1995.
7. P. H. Gregson, Z. Shen, R. C. Scott, V. Kozousek, "Automated Grading of Venous Beading," *Computers in Biomedical Research,* Vol. 28, 291–304, 1995.
8. G. K. H. Fallschlüssel, *Zahnärztliche Implantologie · Wissenschaft und Praxis,* Quitessenz Verlags–GmbH, Berlin, 1986.
9. J. C. Keller, "Dental Implants: The Relationship of Materials Characteristic to Biologic Property," In: J. D. Bronzino, *The Biomedical Engineering Handbook,* CRC Press, Boca Raton, pp. 691–703, 1995.
10. E. R. Daugherty, *An Introduction to Morphological Image Processing,* Tutorial Texts in Optical Engineering, Vol. TT 9, SPIE Optical Engineering Press, Bellingham, 1992.
11. E. R. Daugherty, *Mathematical Morphology in Image Processing,* Marcel Dekker, New York, 1993.

12. J. Serra, *Image Analysis and Mathematical Morphology,* 4th ed., Academic Press, London, 1993.

13. H. J. A. M. Heijmans, *Morphological Image Operators,* Academic Press, Boston, 1994.

14. R. M. Haralick, *Mathematical Morphology,* Tutorial No. 2, IEEE Intern. Conference on Image Processing, 1994.

15. P. E. Danielsson, M. Hammerin, *High accuracy rotation of images,* Report No. LiTH–ISY–I–1152, Department of Electrical Engineering, Linköping University, Sweden, Dez. 1990.

16. P. E. Danielsson, M. Hammerin, "High accurate rotation of images," *CVGIP: Graphical Models and Image Processing,* Vol. 54, pp. 340–344, 1992.

17. P. K. Sahoo, S. Soltani, A. K. C. Wong, "A survey of thresholding techniques," *Computer Vision, Graphics, and Image Processing,* Vol. 41, pp. 233–260, 1988.

18. C. A. Glasbey, "An Analysis of Histogram–Based Thresholding Algorithms," *GVGIP: Graphical Models and Image Processing,* Vol. 55, pp. 532–537, 1993.

19. N. Otsu, "A Threshold Selection Method from Gray–Level Histograms," *IEEE Trans. on SMC,* Vol. SMC–9, pp. 62–66, 1979.

20. U. Welander, P. Nelvig, G. Tronje, W. D. McDavid, S. B. Dove, A. C. Mörner, T. Cederlund, "Basic technical properties of a system for direct acquisition of digital intraoral radiographs," *Oral Surgery Oral Medicine Oral Pathology,* Vol. 75, pp. 506–516, 1993.

21. K. V. Mardia, J. T. Kent, J. M. Bibby, *Multivariate Analysis,* Academic Press, London, 1979.

22. B. Peters, D. Meyer–Ebrecht, T. Lehmann, W. Schmitt, "System analysis fo X–ray–sensitive CCDs and adaptive restoration of intraoral radiographs," *Proceedings of the SPIE,* Vol. 2710, No. 45, this issue.

23. T. Lehmann, C. Goerke, W. Schmitt, A. Kaupp, R. Repges, "A roration–extended cepstrum technique optimized by systematic analysis of various sets of X–ray images," *Proceedings of the SPIE,* Vol. 2710, No. 39, this issue.